Nonlinear Processes in Geophysics (2003) 10: 37–44

Nonlinear Processes in Geophysics

Phase-space holes due to electron and ion beams accelerated by a current-driven potential ramp

M. V. Goldman[1], **D. L. Newman**[1], **and R. E. Ergun**[2]

[1]Center for Integrated Plasma Studies, University of Colorado at Boulder, USA
[2]Laboratory for Atmospheric and Space Physics, University of Colorado at Boulder, USA

Received: 20 December 2001 – Revised: 27 February 2002 – Accepted: 28 February 2002

Abstract. One-dimensional open-boundary simulations have been carried out in a current-carrying plasma seeded with a neutral density depression and with no initial electric field. These simulations show the development of a variety of nonlinear localized electric field structures: double layers (unipolar localized fields), fast electron phase-space holes (bipolar fields) moving in the direction of electrons accelerated by the double layer and trains of slow alternating electron and ion phase-space holes (wave-like fields) moving in the direction of ions accelerated by the double layer. The principal new result in this paper is to show by means of a linear stability analysis that the slow-moving trains of electron and ion holes are likely to be the result of saturation via trapping of a kinetic-Buneman instability driven by the interaction of accelerated ions with unaccelerated electrons.

1 Introduction

FAST (Fast Auroral SnapshoT) satellite measurements have shown the existence of a variety of nonlinear localized electric field structures in the auroral ionosphere. Isolated bipolar field structures have been observed in the downward current region where they have been interpreted in terms of electron phase-space holes moving upward at speeds on the order of electron drift velocities (Ergun et al., 1998) and in the upward current region, where they have been interpreted as ion phase-space holes moving at ion speeds (McFadden et al., 1999). Strong localized unipolar electric fields have recently been measured in the downward current region over distances equal to tens of Debye lengths. Such structures have been interpreted physically as features of diverging electrostatic field structures (sometimes referred to as diverging shocks) in the auroral region (Ergun et al., 2001) and have been shown via numerical simulations (Newman et al., 2001) to be consistent with double layers, which are stationary nonlinear structures well-known from kinetic theory (Block, 1977). Numerical simulations have demonstrated that electron phase-space holes can be produced by an instability involving two electron streams that drive an unstable wave to nonlinear levels where it saturates by trapping the electron streams (Goldman et al., 1999).

Recent 1-D open boundary simulations (Newman et al., 2001) have shown that the double layer provides a means for accelerating one component of electrons relative to another, allowing the two-stream instability to drive waves that grow spatially and develop into electron phase-space holes with distance from the double layer. This picture is also consistent with recent FAST observations (Ergun et al., 2001). In the present paper we report the results of related 1-D open boundary simulations, which confirm the above picture but also lead to new predictions. The main points of this paper and their relation to previous work are as follows:

1. The introduction of a charge-neutral density depression into an initially equipotential current-carrying plasma is shown to result in the formation of a double layer. Whether or not this is the process by which physical double layers form in the auroral region is not known and is probably difficult to determine from satellite studies – although charge-neutral density depressions are not uncommon (Persoon, 1988). Related simulations (Newman et al., 2001) show double-layer formation for weaker initial density depressions than those considered in this paper, suggesting that such density depressions are a potentially robust means for seeding double layers. However, we do not speculate in this paper as to the origins of initial charge-neutral density depressions in the auroral ionosphere.

2. It is confirmed through simulations that the electron phase-space holes evolve nonlinearly from a double layer that accelerates electrons via the two-stream instability. This process has been previously demonstrated numerically by Singh (2000) and by Newman et al.

Correspondence to: D. L. Newman
(david.newman@colorado.edu)

(2001); it is supported observationally by Ergun et al. (2001).

3. A slow-moving train of alternating electron and ion phase-space holes traveling in the direction of the ions accelerated by the double layer is found to form at later times in these simulations. Similar structures were also found in the numerical simulations of Newman et al. (2001) but they are studied in greater detail here. The relevance of this phenomenon to the auroral ionosphere is not yet known. The simulations suggest that downward-moving electron and ion phase-space holes might appear just below the double layer (i.e. on the ionosphere side) in the downward current region. Although there have been no such measurements in the downward current region to date, ion holes have been measured in the upward current region where accelerated ions are also found.

4. A detailed analytical treatment in this paper suggests that the alternating train of slow-moving ion and electron phase-space holes develops out of an electron-ion kinetic instability related to the Buneman instability, which is enabled after ions accelerated by the double layer have traversed many Debye lengths. This analysis has never been presented before to our knowledge. The growth rate, wavenumber and phase velocity of the linearly most-unstable wave are shown to be consistent with the simulations. This agreement supports the hypothesis that the unstable wave traps electrons and ions, leading to the alternating train of slow-moving phase-space holes.

The details of the new simulations are as follows:
A density depression is introduced into an initially stable current-carrying plasma consisting of counterstreaming electron and ion distributions that enter the simulation from opposite boundaries. A potential ramp develops at the location of the density depression as the drifting electrons set up a double layer characterized by spatially separated regions of positive and negative charge density. The potential ramp then accelerates electrons in the direction of their initial drift and the ions (much more slowly) in the opposite direction. In the next stage of evolution, the accelerated electrons participate in a two-stream instability as they interact with "downstream" electrons that are reflected by the potential ramp and are thus confined to the high-potential side of the ramp. The growing wave traps electrons, thereby creating electron phase-space holes moving rapidly in the direction of the accelerated electrons (Goldman et al., 1999). The location of the hole turbulence in relation to the potential ramp, as determined from the simulation, is found to agree reasonably well with recent measurements of hole turbulence in relation to potential ramps found by the FAST satellite in the auroral ionosphere (Ergun et al., 2001). Also in reasonably good agreement are the size of the potential jump in the ramp and characteristics of the electron distribution function.

A new feature found in the simulation at late times is a train of alternating electron and ion holes moving very slowly in the direction of the ion beam. In this paper we present a new theoretical explanation of this feature, which appears in a later stage of evolution – after the *ions* have been accelerated across the initial density depression. We attribute these holes to an electron-ion instability in which the accelerated ion beam interacts with a velocity-steepened hot electron distribution. Such electron-ion instabilities differ from the better-known reactive Buneman instability between cold ions and a cold electron beam. These instabilities are kinetic and arise from Landau-resonant wave-particle interactions. The growth rates are thus smaller than for (fluid) Buneman instabilities. The theoretically-predicted linear growth rate, wavelength and phase velocity of the fastest growing wave all agree fairly well with the properties of the electron-ion hole train seen in phase space in the simulation. This lends support to the interpretation that the train of electron and ion holes arises from ions and electrons trapped in the potential minima and maxima of the unstable wave. This heuristically motivated analysis is only approximate, since the distributions are varying in both space and time. Soon after the appearance of the train of alternating electron and ion holes moving in the direction of the ion beam, a growing stationary hole appears near the base of the potential ramp and eventually accelerates off in the direction of the accelerated electrons, thereby disrupting the potential ramp – at least temporarily. This disruption event may be associated with a localized Buneman instability, although a conclusive determination will require further analysis.

2 Initial conditions, boundary conditions, and development of the potential ramp

The chosen initial and boundary conditions lead to the development of a quasi-stable potential ramp in a 1-D simulation of an initially equipotential current-driven plasma. In the Vlasov simulations described here, the length of the simulation box is 640 λ_e, where the Debye length $\lambda_e = v_e/\omega_e$ is defined in terms of the *initial* electron distribution. The simulation is run for 2500 ω_e^{-1}. (The Vlasov code is described more fully in Newman et al., 2001). The current is maintained at the boundaries by having a drifting Maxwellian electron distribution flow into the simulation box from the left and an oppositely drifting ion distribution flow in from the right (these incoming distributions initially fill the box, except as modified by the imposed density depression discussed below). The incoming distributions are chosen to satisfy the Bohm and the Langmuir conditions (Block, 1977) by taking the electron drift u_e to be equal to the electron thermal velocity $v_e = (T_e/m_e)^{1/2}$ and the ion drift u_i to be equal to minus the ion thermal velocity $v_i = (T_i/m_i)^{1/2}$. The electron and ion temperatures T_e and T_i are taken to be equal, with a ratio of ion to electron mass of $m_i/m_e = 400$.

A local charge-neutral depression with a characteristic width of 80 Debye lengths is introduced as an initial con-

dition at the center of the simulation box. The maximum density depression in the simulation discussed in this paper is 50% of the density at the boundaries. (See Newman et al., 2001, for the shape of a similar density depression that differs only in width and depth.) A current depression is associated with this density depression, although similar results are found when the beam fluxes, and hence the currents, are kept constant in the density depression by locally increasing the drift velocity (Mangeney, 2001; Newman et al., 2001; Carlqvist, 1972). The time for development of a potential ramp is rather sensitive to the depth and spatial width of the density depression, with shallow and/or wide depressions leading to long delays in the appearance of the ramp. Related simulations show that electron phase-space holes can appear even without a well-defined ramp.

A more complicated boundary condition is required for the flux of ions entering from the left boundary and the flux of electrons entering from the right boundary. These fluxes can change with time as growing phase-space holes effectively heat the particles (this is especially true of the electron flux). The distributions at the boundaries are obtained by space-averaging over adjacent narrow layers and are gradually phased in across the width of the layer.

The boundary values of the potential and electric field are both fixed at zero at the left boundary throughout the run while the potential and field are allowed to float at the right boundary with an *initial* value of zero for both. It is important to note that in these simulations there is no initial potential difference between the two boundaries. This is in contrast to other recent "potential-driven" simulations (Singh, 2000), in which both a potential ramp and electron phase-space holes were found.

In our simulations, the potential ramp develops as electrons begin to transit the density depression from one direction and ions from the other (hence, an initial double layer of charge is formed with an associated localized electric field and potential ramp). The magnitude of the potential difference at the two boundaries is determined self-consistently.

3 Evolution of two-stream instability and fast electron phase-space holes

After a short initial transient phase, in which Langmuir waves driven by the initial current inhomogeneity transit and then leave the simulation box, both an incipient potential ramp and the first electron phase-space hole appear. The potential ramp accelerates an electron component moving to the right and reflects the slow electron component moving to the left. Both of these components coexist just to the right of the ramp and constitute a bimodal electron distribution that is unstable to the two-stream instability. It is known that an initial two-stream instability in a homogeneous plasma saturates by creating electron phase-space holes as the growing unstable mode traps the streams (Goldman et al., 1999). In the present simulation, the process occurs in space as well as time and the origin of the spatially localized unstable two-stream instability is now determined by the position of the potential ramp. If the two electron populations have the same density and temperature, the resulting phase-space holes will prop-

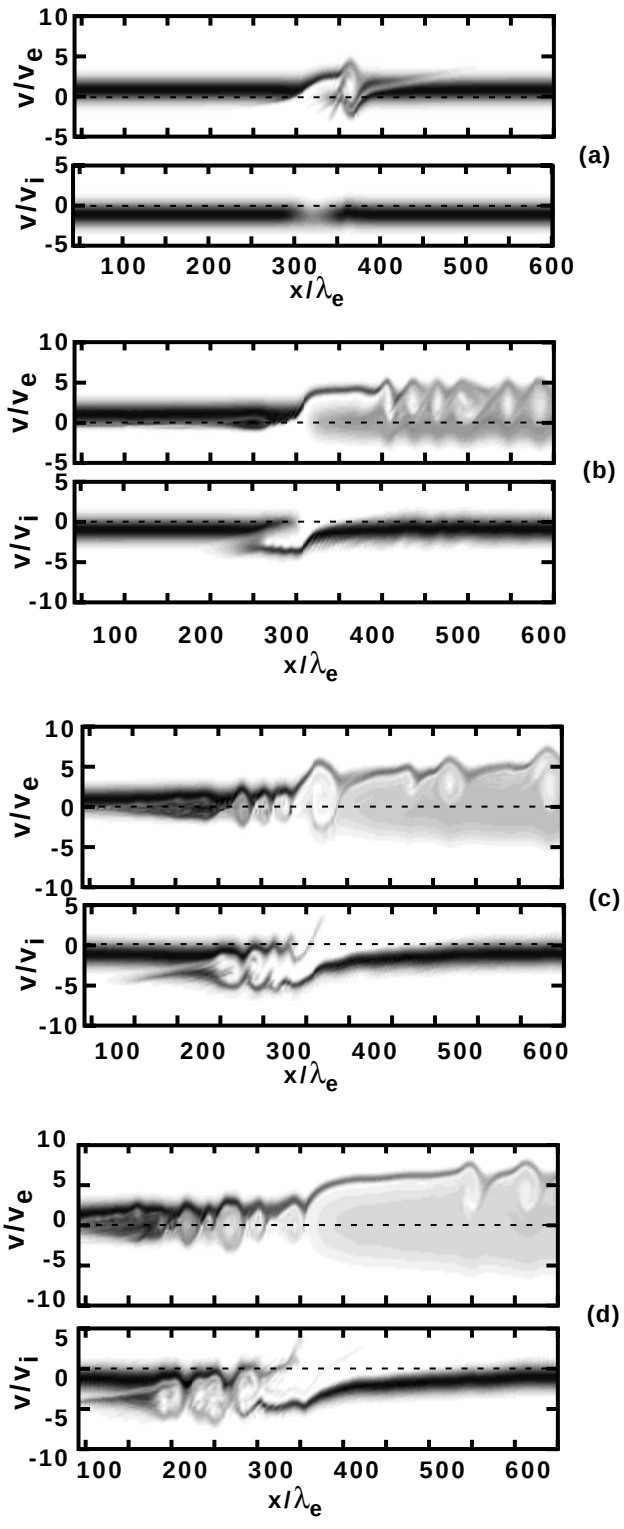

Fig. 1. Phase-space "snapshots" showing $f_e(x, v)$ and $f_i(x, v)$ at four different times: **(a)** $\omega_e t = 45$; **(b)** $\omega_e t = 700$; **(c)** $\omega_e t = 1350$; and **(d)** $\omega_e t = 1712$.

agate at the mean velocity of the total electron distribution which, for this case, is one-half the velocity of the accelerated electrons.

Such fast electron phase-space holes are seen in Figs. 1a and b, which show the behavior of particles in both electron and ion phase space at two early times. At the first time ($\omega_e t = 45$), after the transients have exited the simulation box, the first electron hole is seen to be forming near the center of the box as the accelerated electron beam interacts with the stationary (reflected) component of electrons. The ions have not yet had time to transit the spatial width of the initial density depression. Further to the left and right of the center of the simulation box we can see the original drifting electron and ion distributions, which are stable to electron-ion instabilities.

At the later time of Fig. 1b ($\omega_e t = 700$), we see the effect of a fully-developed stationary ramp in electron phase space. There is a well-defined beam of accelerated electrons occupying a "stand-off" spatial interval to the right of the ramp and to the left of where the holes form. In this interval there is also a component of (reflected) electrons centered at zero velocity, as well as the original drifting ion distribution moving at the slow ion thermal velocity (which scales the velocity axis in the ion phase-space plots of Fig. 1). If we were to view a movie beginning at this time we would see the holes moving off to the right quickly while the ramp remains essentially stationary.

A summary of the time history is shown in Fig. 2, which is a grayscale plot of the dimensionless electric field intensity as a function of space (horizontal axis) and time (vertical axis). Each successive horizontal slice can be regarded as a frame of a "movie." Notable at early times on the right are the fast electron holes moving to the right, which show up as bipolar fields (the shallow slope of the bipolar field structures signifies a large velocity). The double layer ramp field appears as the dark vertical feature near $x = 320\lambda_e$. Other features indicated in Fig. 2 will be discussed later.

By time $\omega_e t = 700$, the ions accelerated towards the left have been able to transit the entire spatial width of the density depression and show up as a well-defined ion beam just to the left of center in Fig. 1b. This marks the beginning of a new stage, seen in Figs. 1c and d, which we interpret in terms of ion-electron beam "Buneman-like" instabilities discussed in the following section.

4 Electron-ion instabilities and slow trains of electron and ion holes

If we look just to the left of the ramp in Fig. 1b, we see a ("cold") ion beam accelerated towards the left, together with "warmer" ion and electron beams. We shall show that this configuration of beams is unstable, and that the evolution from time $\omega_e t = 700$ (Fig. 1b) to just before $\omega_e t = 1350$ (Fig. 1c) is due to an electron-ion instability.

At the later times of Figs. 1c, and d, one can identify spatially-alternating ion holes and electron holes to the left of center, which are moving slowly to the left, in the direction of the ion beam. Thus, the ion hole centers coincide with the electron hole edges, and *vice versa*. The electric fields associated with these holes appear in the time history of Fig. 2 for times $\omega_e t \gtrsim 700$ as the slower train of alternating positive and negative amplitude, which is moving to the left in the region to the left of center. From the slope of the x–t plot, we can estimate the velocity of these structures as $-3.3v_i$, where v_i is the (initial) ion thermal velocity. We shall see that this is slightly slower than the range of velocities of the accelerated ions.

We offer the following tentative explanation for these alternating electron and ion holes associated with the field maxima and minima moving to the left in Fig. 2: By the nonlinear stages seen in Figs. 1c and d, the putative unstable wave has saturated by trapping the particles that drive it – both the slow-moving ions and the slow part of the hot electron beam distribution function. Since ions are trapped in potential minima but electrons are trapped in potential maxima (minima of potential energy), the trapped particles will show up as holes in both electron and ion phase space, as seen in Fig. 1d. We now attempt to quantify this explanation in terms of electron-ion instabilities.

First, we review the properties of electron-ion instabilities. We shall refer to the unstable interaction of an electron beam drifting at velocity v_0 with respect to one or more ion beams as an electron-ion instability (Stringer, 1964; Ahedo and Lapuerta, 2001).

For two cold beams, this becomes a classic textbook example of the standard Buneman instability (Nicholson, 1983): In the frame of the ions, the complex frequency of the fastest growing mode (with wavenumber, $k = \omega_e/v_0$) is given by $\omega = (1 + \sqrt{3}i)(m_e/m_i)^{1/3}$. The growth rate is fast; for our mass ratio of 400 the time for one e-folding is just 8 ω_e^{-1}. The frequency and growth rate are both larger than the ion plasma frequency but smaller than the electron plasma frequency. (For this reason the first order density response is not quasineutral; the electron density response is larger than the ion density response). The phase velocity of this mode is $v_\phi = (v_0/2)(m_e/m_i)^{1/3}$, which is small compared to the relative drift velocity v_0. When the ions are drifting in the direction opposite to the electron beam with velocity v_{ib}, the phase velocity of the unstable mode is reduced by $-v_{ib}$ due to the frame transformation, so that the most unstable linear wave can be stationary or even moving in the direction of the ions.

When one or both of the beams has a sufficiently high temperature, the instability must be treated by kinetic theory (Stringer, 1964) and the growth rate is reduced or even suppressed (i.e. there is no longer instability). A simple kinetic analysis reveals that the initial two drifting Maxwellians in the simulation with $u_e = v_e$ and $u_i = -v_i$ (constituting the current at $t = 0$) are stable against the electron-ion instability (Nicholson, 1983).

However, at time $\omega_e t = 500$ and afterwards, the ion beam to the left of center in Figs. 1b and c has been accelerated by the ramp to such a degree that it is now a "colder" ion beam.

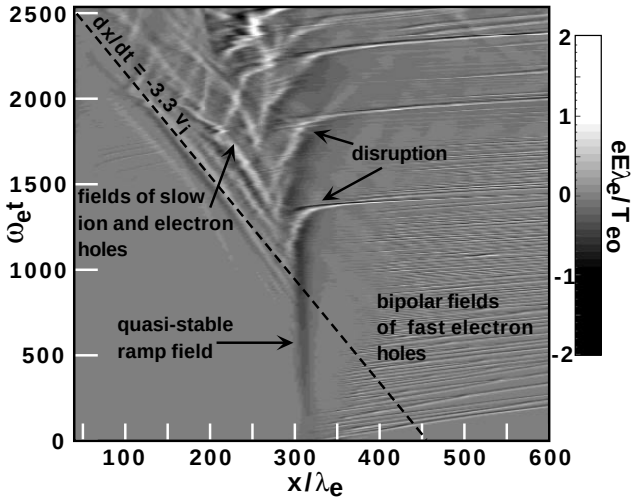

Fig. 2. Time history of the electric field over the duration of the run in the interior of the simulation domain.

The accelerated ion beam interacts with the original and still-present (but modified) electron and ion populations, leading to a slow kinetic electron-ion instability local to the region of the accelerated ions. This instability is enhanced by the distorted hot electron distribution, as we shall soon see. This slow electron-ion instability is related to a Kindel-Kennel (Kindel and Kennel, 1971) instability in one-dimension. The unstable waves are related to ion-acoustic waves, although they are *not* quasineutral. In the ion rest frame their phase velocity is on the order of the ion-acoustic velocity. We will now show that the growth rate, phase velocity and wavelength of such an electron-ion instability are consistent with the simulation stages between the time of Fig. 1b and just before the time of Fig. 1c.

Figure 3 shows the distribution functions $f_s(x, v)$ in electron ($s = e$) and ion ($s = i$) x–v phase space at time $\omega_e t = 904$. The two inner frames are intensity plots of f_e and f_i as in Fig. 1. The outer frames contain "cuts" of the velocity distribution functions near the center of the simulation at equally-spaced locations $\delta x_j = 10 j \lambda_e$, where $j = 0, \pm 1, \pm 2, \ldots$. From Fig. 3, it is clear that there are two distinct ion beams to the left of center (i.e. at $j < -2$), in the region where the ions have been accelerated and where there is a single (distorted) electron beam. In order to determine whether beam-excited wave instabilities in this region can explain the train of alternating ion and electron holes moving slowly to the left, we have fitted analytic functions of velocity to the pair of ion beams and the electron beam at two locations, $j = -4$ and $j = -6$, and have used these analytic distributions in the dielectric function to find linearly unstable modes. Since the ion and electron velocity distributions produced by the simulation in this region have tails, we have used a so-called kappa-distribution (Summers and Thorne, 1991), for $f_s(v)$ for each of the three particle species, $s = e$, $s = i_1$ or $s = i_2$, rather than a Maxwellian. The form of the kappa-distribution function ($\kappa = 1$) is

$$f_s(v) = \frac{2\tilde{n}_s}{\pi \tilde{v}_s} \left[1 + \left(\frac{v - \tilde{v}_{ds}}{\tilde{v}_s} \right)^2 \right]^{-2} . \tag{1}$$

Here the quantities $\tilde{n}_s$, $\tilde{v}_s$, and $\tilde{v}_{ds}$ represent, respectively, the density, thermal velocity, and drift velocity of each of the species (in units of the *initial* electron/ion densities and thermal velocities). These are the three fitted parameters for each distribution. The values of these parameters for the two chosen locations are given in Table 1.

The dispersion relation for kinetic electron-ion instabilities when there are two ion "species" or components and one electron component is given by

$$0 = 1 + \chi_e(k, \omega) + \chi_{i1}(k, \omega) + \chi_{i2}(k, \omega) . \tag{2}$$

The quantities χ_s are the susceptibilities measuring the linear density response of each of the three species. From a linear stability treatment of the Vlasov equation for the distributions given by (1), the susceptibility χ_s for species s takes the form

$$\chi_s(k, \omega) = -\frac{\tilde{\omega}_s^2}{k^2 \tilde{v}_s^2} \left[\frac{\xi_s + 3i}{(\xi_s + i)^3} \right], \tag{3a}$$

$$\xi_s = \frac{\omega - k\tilde{v}_{ds}}{k\tilde{v}_s}, \tag{3b}$$

where $\tilde{\omega}_s = 4\pi n_s e^2/m_s$ is the plasma frequency of species s.

In the so-called "cold plasma" or "fluid" limit characterized by $\xi \to \infty$, the susceptibilities take the usual form, $\chi_s = -\tilde{\omega}_s^2/(\omega - k\tilde{v}_{ds})^2$, which is independent of the thermal velocities v_s. (In this limit, with one cold ion beam and one cold electron beam, the usual fluid Buneman instability is derived.) The slow electron-ion instability is well-known in the literature and is discussed by Davidson (1972) for two cold ion beams and one hot (Maxwellian) electron component. The electron distribution function in the accelerated ion region left of center of phase space is "hot" (with a kappa distribution). Therefore, the two ion beams do not yield susceptibilities that correspond to the "cold plasma" limit. The result of numerically solving Eq. (2) at the two chosen spatial locations are given in Table 2.

The growth rates are smaller than for the cold-electron cold-ion Buneman instability, whose wavelength is also shorter ($k\lambda_e \approx 1$). Waves with the growth rates of Table 1 e-fold roughly six times from the time the ions have traversed the density depression, growing in amplitude by a factor of ~ 400. It is tempting to associate the nonlinearly evolved growing wave in this instability as the source of particle trapping leading to the alternating electron and ion holes seen in Figs. 1c and 1d. This hypothesis is strengthened by the following two additional facts: The phase velocity of the wave is on the order of the velocity of the train of electron and ion holes in phase space ($-3.3 v_i$ according to Fig. 2), since the phase velocity and group velocity of this acoustic-like instability are essentially the same. Furthermore, the wavelength

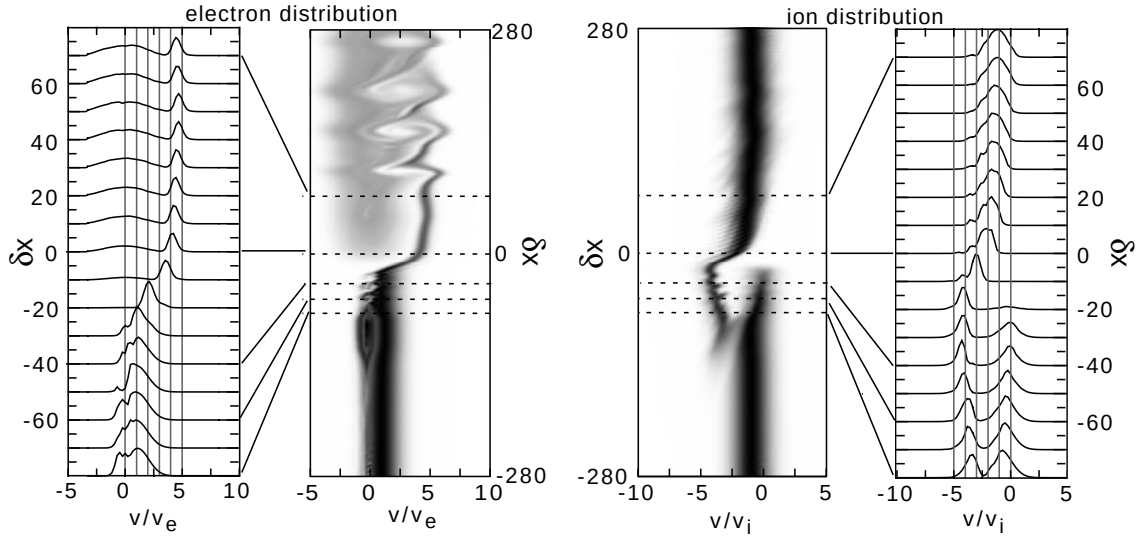

Fig. 3. Electron and ion distributions at $\omega_e t = 904$. The "cuts" (outer frames) map to the region near the center of the distribution-function intensity plots (inner frames) as indicated by the dashed lines connected to a subset of the cuts.

Table 1. Parameters of fits to electron and ion distributions of Eq. (1) for two values of x at $\omega_e t = 904$

Position (δx)	$-40\lambda_e$			$-60\lambda_e$		
	$\tilde{n}_s$	$\tilde{v}_s$	$\tilde{v}_{ds}$	$\tilde{n}_s$	$\tilde{v}_s$	$\tilde{v}_{ds}$
electrons ($s = e$)	0.96	1.60	1.10	1.10	1.70	1.10
fast ions ($s = i1$)	0.31	0.55	−4.25	0.31	0.55	−3.80
slow ions ($s = i2$)	0.33	0.70	0.00	0.42	0.70	−0.50

of the fastest growing wave ($\lambda \approx 2\pi\lambda_e/0.47 \approx 13\lambda_e$) is on the order of the observed hole size.

The hole separation distance in the simulation can be determined from Fig. 1 or from the corresponding electric field or charge density as a function of position. In Fig. 4, we have plotted the difference in density between electrons and ions (in units of the initial density), which is proportional to the charge density, at time $\omega_e t = 904$. The wave structure is already evident with a characteristic wavelength in a range between 0.4 and 0.7 (in units of the *initial* Debye length), although the by-now saturated wave is rather aperiodic. This kinetic instability, like the cold Buneman instability, is not quasineutral; we note from Table 2 that none of the susceptibilities have absolute values significantly larger than one.

There are several reasons why this interpretation of the origin of the slowly moving train of alternating electron and ion holes cannot be more than heuristic in nature: First, the particle distributions are changing fairly quickly in both space and time, both as a result of the acceleration process and due to the evolving trapping potentials. Hence, a linear electron-ion instability analysis based on unchanging characteristic particle drifts and thermal widths cannot be correct except in some average sense. Furthermore, over a very narrow spatial region in the *center* of the potential ramp itself, *both* the electron and ion beams are accelerated and fairly cold, so that the strong, fast Buneman instability may occur in this narrow region (and be likely to require an eigenvalue-eigenfunction treatment).

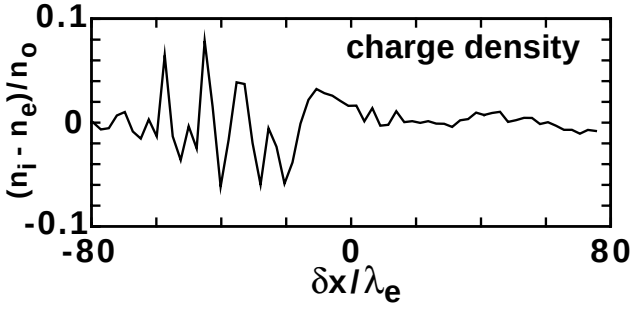

Fig. 4. Charge density $(n_i - n_e)/n_0$ at time $\omega_e t = 904$ near center of simulation box showing non-quasineutral waves with wavenumber $k\lambda_e \approx 0.4$–0.7, which is consistent with the linear stability analysis.

A second difficulty with this interpretation is that this instability occurs over a rather broad range of wavenumbers, so the wave coherence necessary for particle trapping may be hard to achieve without some method of scale selectivity. Selectivity may be provided by the faster Buneman instability in the small range near the center of the simulation cell. Waves would then propagate out of the central region and into the kinetic-Buneman instability region,

Table 2. Properties of most-unstable waves moving to the left at two positions for the distributions of Eq. (1) with parameter values from Table 1

Position (δx)	$-40\lambda_e$		$-60\lambda_e$	
wavenumber ($k\lambda_e$)	0.470		0.470	
growth rate (γ/ω_i)	0.119		0.102	
real frequency (ω/ω_i)	-1.68		-1.49	
phase velocity (ω/kc_s)	-3.57		-3.17	
susceptibilities	$Re(\chi)$	$Im(\chi)$	$Re(\chi)$	$Im(\chi)$
electrons (χ_e)	-0.445	-2.43	-0.246	-2.71
fast ion beam (χ_{i1})	-0.432	2.45	-0.468	2.79
slow ion beam (χ_{i2})	-0.123	0.02	-0.286	-0.08

Table 3. Properties of rightward moving waves at same wavenumber as fastest-growing leftward moving wave in Table. 2

Position (δx)	$-40\lambda_e$		$-60\lambda_e$	
wavenumber ($k\lambda_e$)	0.470		0.470	
growth rate (γ/ω_i)	0.027		0.048	
real frequency (ω/ω_i)	0.323		0.117	
phase velocity (ω/kc_s)	0.687		0.249	
susceptibilities	$Re(\chi)$	$Im(\chi)$	$Re(\chi)$	$Im(\chi)$
electrons (χ_e)	0.09	-2.98	0.24	-3.12
fast ion beam (χ_{i1})	-0.06	0.00	-0.09	0.01
slow ion beam (χ_{i2})	-1.03	2.98	-1.15	3.11

where their growth rate decreases. In the kinetic region, the broader range of wavenumbers corresponding to growing waves would permit amplification of the already partially grown waves from the unstable region near the center, where the electrons have a larger drift with respect to the ions.

We note from the susceptibility values in Table 2 that the slow ion beam (with drift velocity close to zero) essentially does not participate in this instability. The instability is driven mainly by the interaction of electrons with the ion beam at $-4.25v_i$. If the slow ion beam is left out of the dispersion relation, the properties of this instability are essentially unchanged. However, there is another unstable root to the dispersion relation in Eq. (2). At the same wavenumber as in Table 2 (i.e. $k\lambda_e = 0.470$), this root has a lower growth rate of about 40% of the fast-ion-beam instability, as seen in Table 3. The phase velocity of this more slowly growing mode is positive but it cannot travel very far because the slow ion beam is reflected by the double layer field and disappears just to the right of its reflection point near $\delta_x = -20\lambda_e$ (see Fig. 3).

Finally, we remark that the disruption of the double layer evident around time $\omega_e t = 1350$ in both Fig. 1 and Fig. 2 is initiated by the appearance of a giant electron hole that spins in place before accelerating to the right and destroying the double layer. Thus, not only does the double layer lead to the creation of phase-space holes but it appears that holes can react back on the double layer, thereby influencing its lifetime. It seems likely that there is once again an underlying instability, probably of the Buneman variety, since the center of the disrupting hole is slowly moving or stationary for a while before moving off quickly to the right. The lifetime of the double layer in this simulation is on the order of $1000\omega_e^{-1}$, a value that probably depends on the ion mass. Since $m_i = 400m_e$ in these simulations (smaller by a factor of almost 80 than the mass of oxygen, which can be the dominant ion species in the auroral ionosphere), the lifetime of the double layer with the physical ion mass should be correspondingly longer. Other factors, such as details of the initial distribution functions, could also affect the longevity of the double layer.

5 Conclusions

New 1-D open-boundary Vlasov simulations of a current-carrying plasma with an initial density depression but no initial electric field show the development of many different kinds of spatially-localized electric fields. At early times, the flow of a higher density of electrons *into* the density depression and a lower density of electrons *out of* the density depression creates the charge separation which leads to a potential ramp (corresponding to both a localized electric field and a double layer of total charge density). Subsequently, electrons are accelerated by the potential ramp into a higher velocity beam which interacts with the slow electron component consisting of electrons both incident from the opposite direction and reflected by the ramp. This leads to a two-stream instability, which saturates by trapping both the fast (accelerated) and the slow electron components. In electron phase space, this shows up as a series of *holes* that can merge with one another and that grow in size as the double layer develops. The unipolar electric field of the quasistationary

double layer and the turbulent bipolar electric field of the electron holes are consistent with recent observations (Ergun et al., 2001; Newman et al., 2001).

The focus of the present paper, however, has been on localized field structures moving slowly to the left, which appear later after the ions have been accelerated by the potential ramp of the double layer in the *opposite* direction to that of the accelerated electrons. The new localized field structures appear to arise from a kinetic instability, related to the Buneman instability, in which an ion beam interacts with an electron beam to produce a wave moving almost at the ion velocity. The growth rate, wavenumber and phase velocity of the unstable waves obtained from a linear stability analysis all are consistent with the simulation results. These slow waves then saturate by trapping both electrons and ions, leading to a train of alternating electron and ion phase space holes moving at a slightly slower velocity than the accelerated ions, as observed in the simulation at late times. Such nonlinear wave trains have not yet been observed in the downward current region of the auroral ionosphere. In that context they would lie close to the double layer and would be moving slowly Earthward. However, ion beams and ion holes *have* been observed in *upward* current regions (McFadden et al., 1999), and these results may be relevant there, although ion-ion instabilities are another possible hole-producing mechanism (Børve et al., 2001). It should be stressed that our simulation studies need to be extended to higher dimensions where competing processes, such as electrostatic ion cyclotron harmonic instabilities, occur on the ion time scale. Even without such processes, ion holes may be less robust in higher dimensions if the ions are weakly magnetized with $\Omega_i/\omega_i \ll 1$ (Morse and Nielson, 1969). Indeed, the ion holes observed in the upward current region are found where the plasma density is lower (hence,the ratio Ω_i/ω_i is larger), possibly leading to magnetic stabilization of the ion holes as found in recent simulations (Børve et al., 2001; Daldorff et al., 2001).

Finally, we have seen that the lifetime of the double layer in our simulation is determined by the appearance of a giant hole that is initially slowly moving or stationary. This hole may also arise from a Buneman instability, although some of its properties are highly nonlinear. The lifetime of the double layer in the simulation is found to be on the order of $1000\omega_e^{-1}$, although a more realistic ion mass and effects of higher dimensions could change this result.

Acknowledgements. This research was supported by grants from NSF (ATM-9802209), NASA (NAG5-9026) and DOE (DE-FG03-98ER54502).

References

Ahedo, E. and Lapuerta, V.: Comparison of collisionless macroscopic models and application to the ion-electron instability, Phys. Plasmas, 8, 3873–3878, 2001.

Block, L. P.: A double layer review, Astrophys. Space Sci., 55, 59–83, 1977.

Børve, S., Pécseli, H. L., and Trulsen, J.: Ion phase-space vortices in 2.5-dimensional simulations, J. Plasma Phys., 65, 107–129, 2001.

Carlqvist, P.: On the formation of double layers in plasmas, Cosmic Electrodynamics, 3, 377–388, 1972.

Daldorff, L. K. S., Guio, P., Børve, S., Pécseli, H. L., and Trulsen, J.: Ion phase space vortices in 3 spatial dimensions, Europhys. Lett., 54, 161–167, 2001.

Davidson, R. C.: Methods in Nonlinear Plasma Theory, Academic Press, New York, 1972.

Ergun, R. E., Carlson, C. W., McFadden, J. P., Mozer, F. S., Delory, G. T., Peria, W., Chaston, C. C., Temerin, M., Roth, I., Muschietti, L., Elphic, R., Strangeway, R., Pfaff, R., Cattell, C. A., Klumpar, D., Shelley, E., Peterson, W., Moebius, E., and Kistler, L.: FAST satellite observations of large-amplitude solitary structures, Geophys. Res. Lett., 25, 2041–2044, 1998.

Ergun, R. E., Su, Y.-J., Andersson, L., Carlson, C. W., McFadden, J. P., Mozer, F. S., Newman, D. L., Goldman, M. V., and Strangeway, R. J.: Direct observation of localized parallel electric fields in a space plasma, Phys. Rev. Lett., 87, 045 003, 2001.

Goldman, M. V., Oppenheim, M. M., and Newman, D. L.: Nonlinear two-stream instabilities as an explanation for auroral bipolar wave structures, Geophys. Res. Lett., 26, 1821–1824, 1999.

Kindel, J. M. and Kennel, C. F.: Topside current instabilities, J. Geophys. Res., 76, 3055, 1971.

Mangeney, A.: private communication, 2001.

McFadden, J. P., Carlson, C. W., and Ergun, R. E.: Microstructure of the auroral acceleration region as observed by FAST, J. Geophys. Res., 104, 14 453–14 480, 1999.

Morse, R. L. and Nielson, C. W.: One, two, and three-dimensional simulation of two-beam plasmas, Phys. Rev. Lett., 23, 1087–1090, 1969.

Newman, D. L., Goldman, M. V., Ergun, R. E., and Mangeney, A.: Formation of double layers and electron holes in a current-driven space plasma, Phys. Rev. Lett., 87, 255 001, 2001.

Nicholson, D. R.: Introduction to plasma theory, Wiley, New York, 1983.

Persoon, A. M.: Electron density depletions in the nightside auroral zone, J. Geophys. Res., 93, 1871–1895, 1988.

Singh, N.: Electron holes as a common feature of double-layer-driven plasma waves, Geophys. Res. Lett., 27, 927–930, 2000.

Stringer, T. E.: Electriostatic instabilities in current-carrying and counterstreaming plasmas, Plasma Phys., 6, 267–279, 1964.

Summers, D. and Thorne, R. M.: The modified plasma dispersion function, Phys. Fluids, B3, 1835–1847, 1991.